Eur. Phys. J. B **51**, 593–600 (2006)
DOI: 10.1140/epjb/e2006-00247-1

THE EUROPEAN PHYSICAL JOURNAL B

Linear and nonlinear optical properties of hydrated and dehydrated silica micro-spheres under an electric bias

C.P. Pang and J.T. Lue[a]

Department of Physics, National Tsing-Hua University, Hsin-Chu, Taiwan

Received 19 January 2006 / Received in final form 18 April 2006
Published online 22 June 2006 –

Abstract. The linear refractive indices and nonlinear second-order susceptibility of hydrated and dehydrated silica micro-spheres are studied using attenuated total reflectance (ATR) and the second harmonic generation (SHG) method in direct transmission, respectively. A dramatic change of the effective dielectric constant of silica suspension under an electric bias was observed, which is attributed to particle redistribution in the fluid. Dielectric constants of dehydrated silica spheres change slightly under an electric field due to Pockels effect, for which we measure a linear electro-optical coefficient of $r_{33} \sim 3.4 \pm 0.7$ pm/V. The transmission second harmonic generation comes from the third-order susceptibility $\chi^{(3)}$, which is a coupling of two photons and the electrostatic field induced by the surface –OH charges as characterized by the Gouy-Chapman model. The SH signal from the dehydrated silica vanishes because of the loss of –OH groups on the particle surfaces. Dehydration of silica beads is irreversible. The optical properties of dried silica spheres do not recover their original hydrated state when distilled water is added.

PACS. 42.65.Ky Frequency conversion; harmonic generation, including higher-order harmonic generation – 73.20.Mf Collective excitations (including excitons, polarons, plasmons and other charge-density excitations) (for collective excitations in quantum Hall effects, see 73.43.Lp) – 78.66.Vs Fine-particle systems

1 Introduction

Fused silica is widely distributed across the earth. The interface of amorphous silica plays important roles in catalysis, chemical reactions and micro electronic fabrication. A meticulous study of the properties of amorphous silica surfaces is crucial if this most pervasive of materials is to be used in practical applications.

Pockels effect addresses the change of the refractive index under an applied electric field, which offers practical application in modulators and optical switches. In general, Pockels effect exists in non-centrosymmetric crystals and is proportional to the second-order susceptibility. The demonstration of an electro-optic modulator effect [1] in inversion symmetry silica-spheres suggests a new field of this effect in active silica-based integrated optics and fiber devices.

Attenuated total reflection (ATR) is a prominent method for probing dielectric constant changes in the underlying material by excitation of surface plasmons. The angular position of the minimum dip of an ATR curve crucially depends on the dielectric constant of the medium adjacent to the metal film. Either the Kretschmann-Raether or the Otto configuration [12] can be implemented to generate surface plasmons and to detect a small change in the refractive index of silica micro-spheres induced by the applied electric fields. In this work, we use the Kretschmann-Raether configuration as shown in Figure 1 to measure the Pockels coefficient of silica spheres.

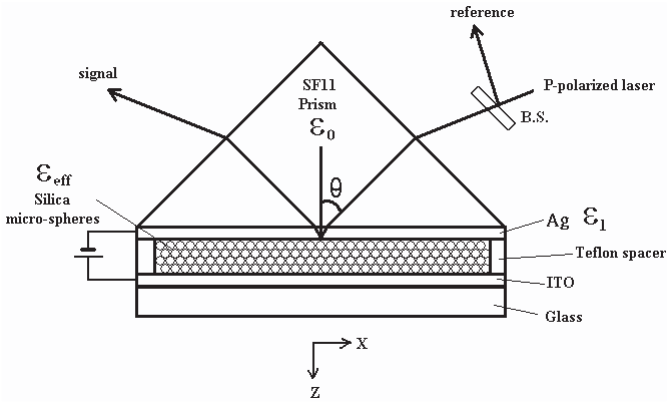

Fig. 1. The Kretschmann-Raether configuration for the ATR experiment.

Nonlinear optics has become a very powerful tool for the surface and interface diagnostics of surface structure reconstruction and adsorption of molecules. This technique relies on the fact that the inversion symmetry of the crystal structure is interrupted at the interface, which coincides with a strong electric field gradient. For media

[a] e-mail: jtlue@phys.nthu.edu.tw

behaving with inversion symmetry like amorphous silica, SHG is forbidden in the bulk but allowed on the surface or interface where impurity ions are absorbed, resulting in strong anharmonic bonds. Since the first report [2] that revealed the existence of a large, permanent second-order nonlinearity $\chi^{(2)}$ in bulk fused silica induced by thermal poling, many groups have investigated the nonlinear properties of this omnipresent material. The majority of the nonlinear optical studies on the silica interface have been conducted on planar, nonporous silica glass/quartz surfaces. These results may, however, not fully reflect the surface structure and reactivity of silica gels or powders. In recent years, SHG from centro-symmetric spherical particles has gained a lot of attention both theoretically [3–6] and experimentally [6–10] because nanofabrication techniques are now capable of producing nanoparticles with controlled size and structures. For example, the nonlinear optical properties of these structures are used to measure the spatial and temporal distribution of charges on water droplets in thunderclouds [11].

In this work we attempt to describe the effect of dehydration and re-hydration of silica micro-spheres, dispersed originally in water, on the intensity of transmitted SHG. We attempt to elucidate the relationship between the change of refractive indices and enhancement of SHG of fused silica micro-spheres.

2 Theory

2.1 Excitation of surface plasmons

The quantitative description of the minimum of the attenuated totally reflected (ATR) intensity in the Kretcshmann-Raether configuration can be derived by the Fresnel equation for the three-layer system i.e. 0/1/2 where 0 specifies the SF11 prism, 1 is the silver film of thickness d, and 2 is the dielectric layer, respectively. Denoting the incoming field by E_0, the outward field by E_r, then the reflectivity R of the p-polarized light is given [12] by

$$R = |r^p_{012}|^2 = \left|\frac{E^p_r}{E^p_0}\right|^2 = \left|\frac{r^p_{01} + r^p_{12}e^{2ik_{1z}d}}{1 + r^p_{01}r^p_{12}e^{2ik_{1z}d}}\right|^2,$$

with

$$r^p_{ij} = \left(\frac{k_{iz}}{\varepsilon_i} - \frac{k_{jz}}{\varepsilon_j}\right) \Big/ \left(\frac{k_{iz}}{\varepsilon_i} + \frac{k_{jz}}{\varepsilon_j}\right), \tag{1}$$

where k_{iz} is the wave vector along the normal of the surface in the ith medium. Taking $n_0 = 1.77373$ for SF11 prism at$\lambda = 679.5$ nm at 25 °C [13], and $\varepsilon_1 = -21 + 0.84i$ [12], $d = 55$ nm, we can simulate the ATR spectrum by equation (1). The effective refractive index of the dielectric layer 2 can be readily derived from the fitting of the experimental data.

2.2 The linear electro-optic effect

Without considering the anisotropy of an electro-optic material, the relation between the refractive index and the applied electric field is given by

$$n(E) = n_0 + aE + bE^2 + \ldots \tag{2}$$

where a and b are coefficients of the first-order and second-order terms, respectively. The linear electric field dependence term, $\Delta n = n(E) - n_0$, arises from Pockels effect. We may express the refractive index, equation (2), by

$$n(E) = n - \frac{1}{2}rn^3E + \frac{1}{2}\varsigma n^3E^2 + \ldots \tag{3}$$

Typical values of r range from 1 to 100 picometers/volt. It is related to the nonlinear susceptibility by $r = 2\chi^{(2)}(-\omega;\omega,0)/n^4$ [14], where $\chi^{(2)}$ is the second-order nonlinear susceptibility.

When a poling field normal to the sample surface is applied, an axis of isotropic symmetry with mirror plane is created. Consequently, the modified indices of refraction are given by

$$n'_x = n'_y = n_0 - n_0^3 r_{13}E/2, \tag{4a}$$

$$n'_z = n_0 - n_0^3 r_{33}E/2, \tag{4b}$$

where n_0 is the refractive index without bias.

Referring to our previous study on Ferro fluids, the excited surface plasmons interact strongly with magnetic ellipsoids that aggregate under an external magnetic field with their long axis parallel to the normal direction of the metal film [15]. Therefore, with the electric field normal to the metal plane, we measured the coefficient r_{33} in this work.

2.3 Second harmonic generation

The second-order nonlinear polarization can be expressed as

$$P^{(2)} = \chi^{(2)}E_\omega E_\omega, \tag{5}$$

where E_ω is the incident optical field at frequency ω. For centro-symmetric media such as fused silica, $\chi^{(2)} = 0$. However, a DC polarization by an external field can induce a third-order nonlinear polarization $P^{(3)}$, which can also generate the SH as

$$E_{2\omega} \propto P^{(3)}_{2\omega} = \chi^{(3)}E_\omega E_\omega \phi', \tag{6}$$

where $\chi^{(3)}$ is the third-order nonlinear susceptibility and ϕ' is the static field. The SHG can be contributed from the third order susceptibility $\chi^{(3)}$ along with an electrostatic field ϕ'.

On the surface, a surface potential $\phi(0)$ is induced by the surface charges which can be calculated through the Gouy-Chapman model [16] to yield

$$\phi(0) = \frac{2kT}{Z}\sinh^{-1}\left[\sqrt{\frac{\sigma^2\pi}{2\varepsilon kTC}}\right], \tag{7}$$

where C is the total bulk electrolyte concentration, k is the Boltzman constant, T is the temperature, Z is the valence of the ions, σ is the surface charge density of particles, and ε is the dielectric constant of the bulk solution.

3 Sample preparation and experimental procedures

The silica spheres of diameter 0.99 ± 0.05 μm suspended in an aqueous solution with 2 wt% were purchased from Duke Scientific Corporation (catalog number 8100). The spheres have densities varying from 1.8 to 2.2 g/cm^3. The fluid is filled in a glass cell with the inner surface deposited of indium-tin-oxide (ITO) film to study the effect of electric fields on optical properties. It should be noted that commercially available ITO glass generates a strong SH signal. To remove this background noise, we prepared the conducting amorphous ITO films by DC sputtering in argon gas, which gives a null SHG signal as shown in Figure 8. A Teflon sheet of 25 μm thickness was used as the spacer.

Two approaches were used to study the linear optical properties of silica micro-spheres. Firstly, the fluid suspended with silica spheres is directly filled into the electrode cell. Secondly, the dehydrated silica spheres are deposited on ITO plates by a method of so-called "vertical deposition" [17,18]. The ITO plates were vertically immersed in a fluid suspension of silica spheres, which were heated slowly to about 80 °C. Due to capillary force and surface tension, a meniscus surface forms between the suspension and the ITO plate, where the solvent evaporated from the freshly deposited silica spheres becomes the driving force for the convective transfer of spheres to be deposited. Figure 2 shows an example of a deposited monolayer of silica spheres on a cover glass. By adjusting the slope of the substrate immersed in the suspension, we can deposit a multilayer sample.

The experimental set-up for the SHG measurement is sketched in Figure 3 [19]. The source of the fundamental radiation is a passively mode-locked, Q-switched Nd:YAG laser with a typical FWHM of 100 ps at a Q-switch repeating rate of 1 kHz. The laser light passes through a glass beam splitter, which reflects 5% of the laser intensity on an AT-cut quartz plate, which is employed as the reference SHG standard. The straight beam, on passing through a Schott glass filter, illuminates the sample. The transmitted light then passes through a set of blocking filters, which only allow the SH wave to pass through. The SHG signal is detected by a photomultiplier tube and then recorded by a gated counter. Due to the narrow pulse width, the single-pulse energy was reduced to as low as 0.3 mJ to avoid thermal destruction. In this experiment, the dehydrated silica micro-spheres were illuminated by a focused laser beam, with a spot size of $\sim$0.5 mm^2, while the hydrated sample was illuminated by an expanded beam, with a spot size of $\sim$2 mm^2, to avoid laser dehydration.

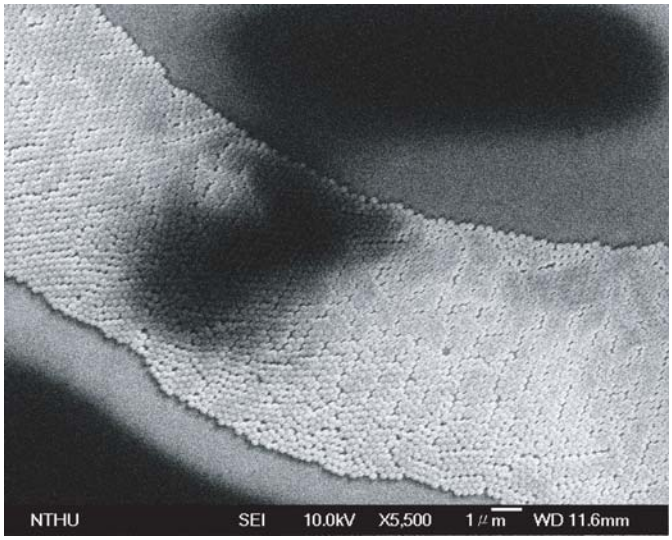

Fig. 2. SEM photograph of a monolayer of silica micro-spheres deposited on a cover glass.

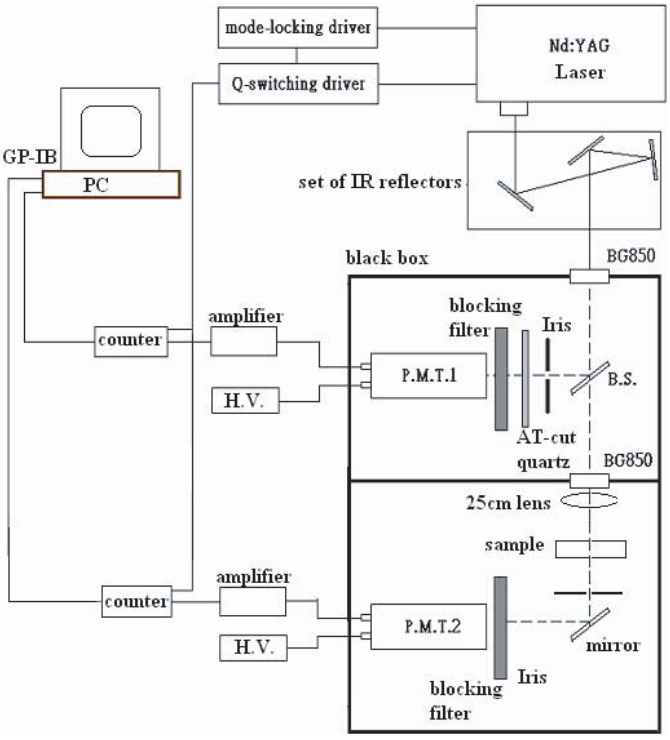

Fig. 3. The setup for the SHG experiment.

4 Results and discussion

4.1 Linear Pockels effect

For hydrated silica micro-spheres, the angular positions of the ATR dips shift to larger angles when the applied electric field increases as shown in Figure 4. The effective dielectric (ε_{eff}) of the medium just contacting the silver film increases with the applied fields to a saturation value at 1.2×10^5 V/m. Surface plasmons decay exponentially along the wave propagating direction, and crucially depend on the index of the medium intimately contacting the metal film. This result suggests that the suspended silica spheres are attracted to the silver electrode. The saturation phenomenon can be explained by the agglomeration of more and more polarized silica spheres on the silver film as the

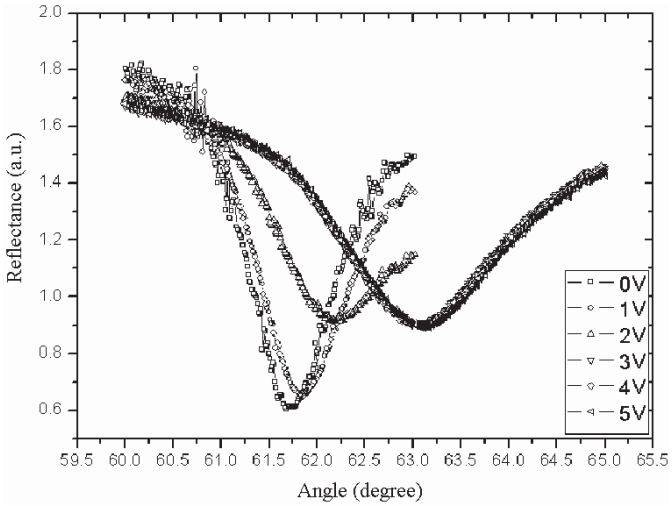

Fig. 4. The ATR curves for silica spheres suspended in water under various electric biases. The ATR dips shift dramatically to larger angles and are then stationary for applied voltages larger than 3 V (corresponding to an electric field of 1.2×10^5 V/m).

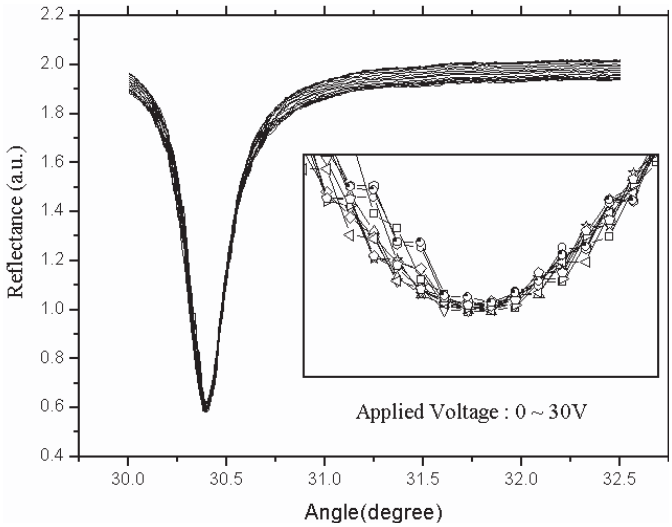

Fig. 5. The ATR curves for silica spheres deposited on an ITO glass attached to the bottom of an Ag-coated prism, under a bias from 0 to 30 V at an angular resolution of 0.01 degree. The insert for the exaggerated curves clearly indicates no shift of ATR dips at various biases.

electric field increases to make a larger effective refractive index of the mixed medium. This redistribution of silica spheres can be confirmed by examining in situ microscope observation, as shown below in Figure 10.

For the ATR experiment of dehydrated silica microspheres, we deposited a monolayer of silica spheres on the ITO plate and attached it to a silver-coated prism. As shown in Figure 5, the ATR dips are not shifted under a wide range of electric biases (from 0 to 30 Volts). The positions of dips infer that beneath the silver surface is air. The silica spheres are not attached to the silver film and the surface plasmons occur on the interface of silver

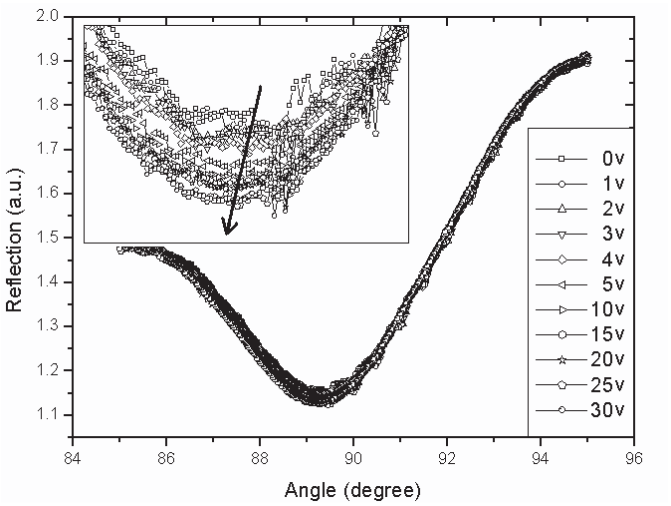

(a)

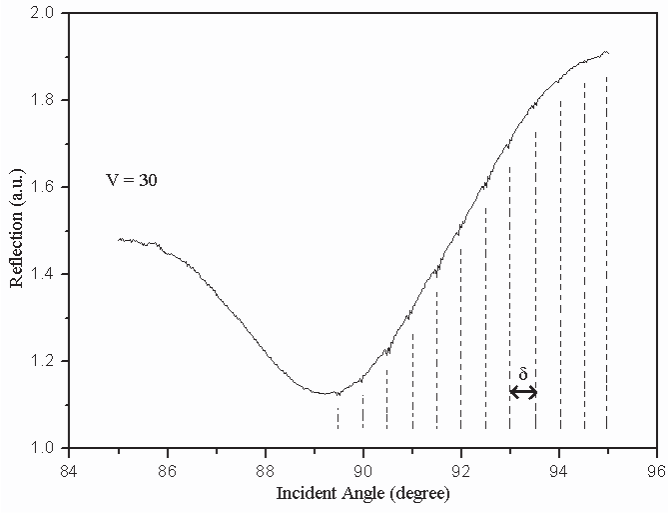

(b)

Fig. 6. (a) The ATR curves for silica spheres directly deposited on the silver-coated prism-base. The insert reveals a slightl shift of ATR dips under different electric fields. (b) Periodic dip within the typical ATR dip indicating extra coupling factor due to surface plasmons resonance.

and air. We also deposited a monolayer of silica spheres directly on the silver surface. In this case, the ATR dips shift slightly when the applied field increases to as large as 3×10^7 V/m as shown in Figure 6a.

Figure 7 shows the effective refractive indices of the silica array, obtained by fitting the ATR curves to the Fresnel equation, under various biases. The effective-index shift can be elucidated merely by the presence of silica beads under bias since there is no evidence of the effect by air as seen in Figure 5. Consequently Figure 7 demonstrates the linear electro-optic effect of silica spheres. The electro-optic coefficient r_{33} obtained in this experiment in accord with equation (4b) is $\sim 3.4 \pm 0.7$ pm/V, which is about ten times larger than the reported value [20] for the thermally poled planar fused-silica.

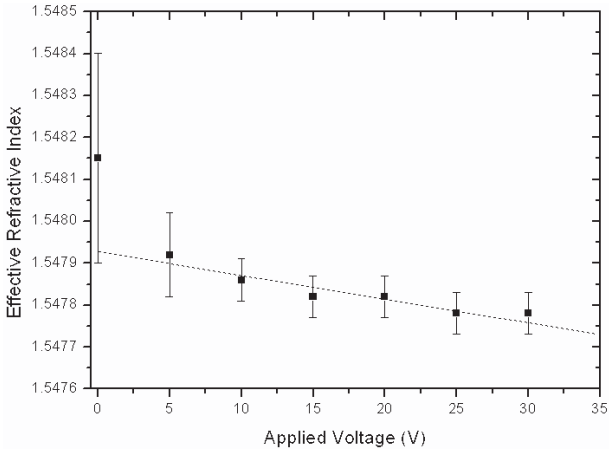

Fig. 7. A linear dependence of refractive index on electric field for silica spheres gives a Pockels coefficient $r_{33} \sim 3.4 \pm 0.7$ pm/V.

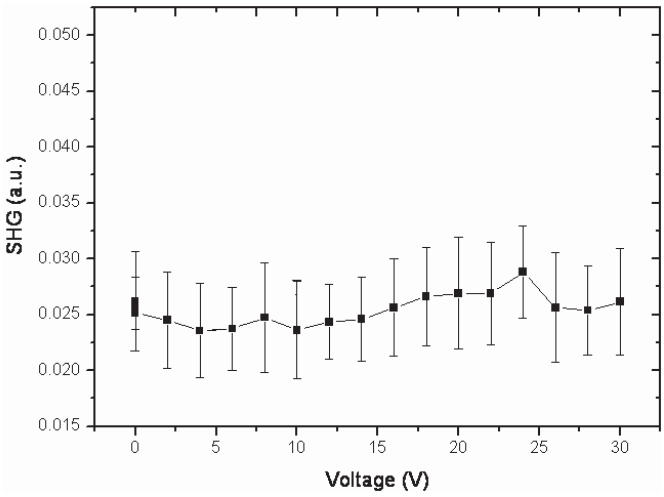

Fig. 8. The transmitted SHG from the cell originally filled with dehydrated silica spheres and then refilled with water under various biases. No transmitted SHG is found. The null result is also found for samples of (1) the empty ITO cell, (2) the cell filled with de-ionized water, and (3) the cell filled with dehydrated silica spheres.

It is worth noting that sharp spikes occur periodically as the incident angle increases to larger than the ATR dip angle as shown in Figure 6b. This phenomenon cannot be explained by the interference reflecting from parallel plates as discussed in reference [21], which should be violently oscillating spikes occurring at incident angles smaller than those for the ATR dip. We have assumed here that this nearly negligible periodic spike is due to the excitation of the surface plasmons on the regularly arrayed silica-spheres, which evoke an additional Bragg wave vector for the phase matching condition.

4.2 Nonlinear harmonic generation

Before trying SHG of the silica-bead suspension, we first examined the SHG from pure water, dried and re-hydrated

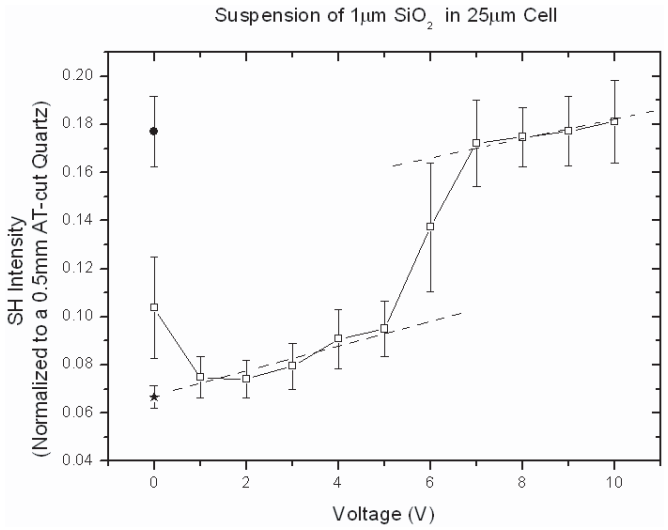

Fig. 9. Transmitted SHG from silica micro-spheres suspended in water under different electric fields. A typical error bar is illustrated at $V = 0$. The SH intensity first decreases slightly and then increases dramatically at $V = 6$, and then is saturated for voltages larger than 10 V. The SH intensities after turn-off of the voltage at the original place and at other places are shown as a filled circle and a filled star, respectively.

dried silica-spheres. As depicted in Figure 8, they all illustrate negligible signals even under an applied field over 30 Volts/50 μm.

The SHG from the silica sphere suspension under an electric field is depicted in Figure 9. The SH signal first drops a little and then grows dramatically at a bias near 6 Volts. There are two linear regions as shown in the fitted dash-lines. After the bias was turned off, the SH intensity remains at an almost constant value, as given by the filled circle in Figure 9. We also measured the SH intensity at an un-illuminated region after turning off the bias as given by the filled star in Figure 9, which is weaker than that at starting bias. This implies that SHG from the polarized silica spheres is expedited by light illumination.

Figure 10 shows the optical microscopy images of the silica suspension cell before and after laser illumination. Figure 10a shows silica spheres suspended freely in pure water before applying an electric field. Image blur is due to the diffraction and Brownian motion of particles. Figure 10b, the image focusing on the rear electrode, illustrates that silica spheres after laser illumination under an electric bias (which are subjected to an anchor effect) are stable, which gives a sharp image. The agglomeration increases with applied field. The silica spheres are splashed away by the laser radiation on the front electrode as shown in Figure 10c. The illuminated cell is sketched in Figure 10d.

No transmitted SHG was observed from pure water or dried silica spheres. SHG from silica bead suspension should come from the interface between silica and water. However, no transmitted SHG was observed from dehydrated silica beads refilled with water, implying that the SHG source is the –OH group that was lost during

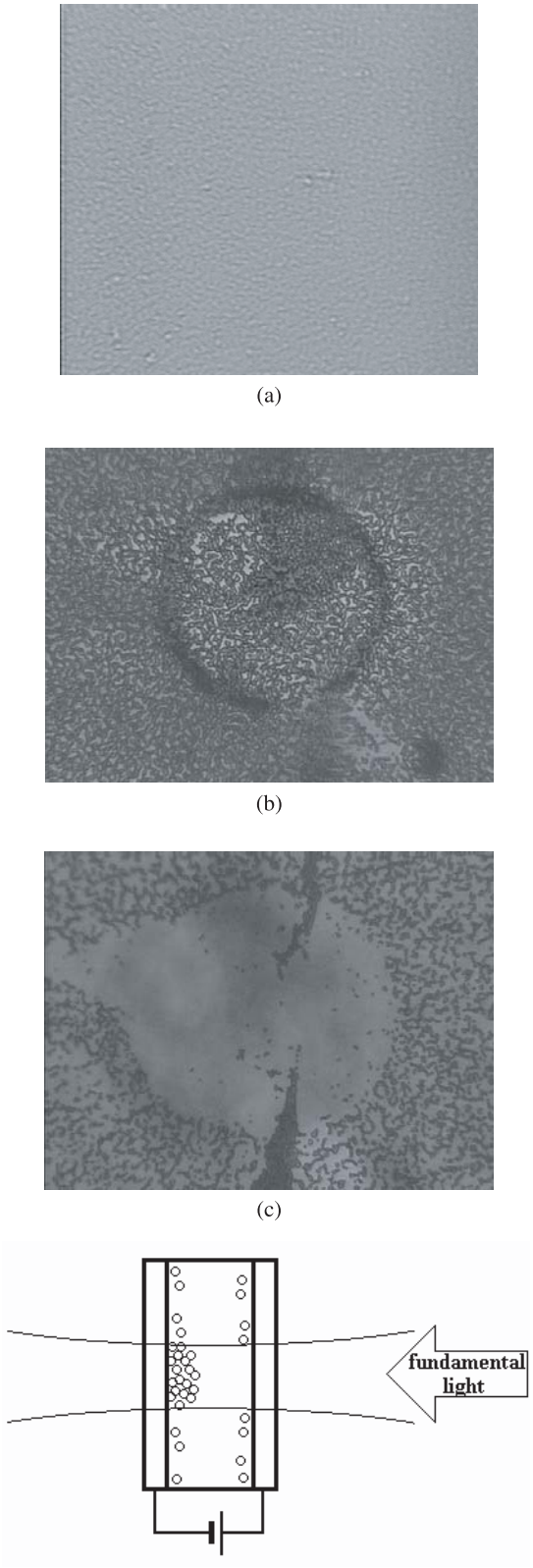

Fig. 10. Optical microscopic pictures of the fluid embedded with silica micro-spheres for light focused on various parts of the cell: (a) before light illumination, (b) after illumination at the rear electrode side, (c) on the front electrode side, and (d) diagram showing the cell structure and light direction.

dehydration. Lost –OH groups cannot be regained simply by adding water to dehydrated silica.

Since 1950, researchers have been involved in developing various methods to investigate the water/silica interface. Many methods concerning the dehydration of silica have been reported but few give accurate assessment of the degree of de-hydroxylation of the silica surface. The inconsistency of the data is pervasive since silica demonstrates diversified structure, and is readily embedded with various traces of impurities. Dehydration data are difficult to reproduce because water vapor strongly catalyzes rearrange into siloxane bonds. Up until the 1980s, few dehydration and re-hydration studies of silica surfaces were performed because of the difficulty of obtaining completely hydrogen-free, and finely divided silica with sufficient uniformity and high specific surface area. Synder [22] reported that re-hydration of the partly dehydrated-siloxane surfaces, even when embedded in water, is exceedingly slow at 25 °C. Agzamkhodzhaev et al. [23] showed that the more completely the surface was dehydrated, the longer the time required for re-hydration. For example, a surface dehydrated at 900 °C for 10 hrs to an OH^- ion density of 0.06 nm^{-2} required several years to become re-hydrated even embedded in water at room temperature. In this sense, the dehydration of silica is almost irreversible. Our results are compatible with this statement. The optical properties of silica spheres for those suspended in water and dehydrated are quite different.

Incoherent second-order light scattering originating from the density and orientation fluctuations of molecules has been observed in bulk centrosymmetric media. However, this emission is not charge or bias dependent and hence cannot account for our results. Harmonic generation from bulk second-order nonlinearity $\chi^{(2)}$ also cannot explain the present result since it vanishes in the forward direction. This explains the reason why no transmitted SHG from dehydrated-silica micro-spheres was detected even though the ATR result shows that silica spheres have a large value of r_{33}.

Considering the SHG from isolated micro spheres, either of neutral or with permanent surface charge, forward emission is forbidden from the view point of theoretical calculations [3–6], and from experimental results [9,11,24]. In the Mie scattering for $ka \geq 1$, the SH intensity peaks occur at 10° and 170° whilst they vanish in the forward direction [6]. It should be noted that although forward SH emission can not be explained by isolated droplets, multiple-scattering can easily take place resulting in the forward SH emission. Comparing the SH intensity at the un- and illuminated place, a multiple-scattering model cannot account for our result.

In our case, the forward SH emission is linearly proportional to the external electric field in conjunction with irradiation. It is reasonable to assume that such SH emission is from 3rd order nonlinearity $\chi^{(3)}$, which is a coupling of two photons and an electrostatic field, as given in equation (6). The electrostatic field here is the surface potential, as described in equation (7), which can be enhanced by an external field together with irradiation to

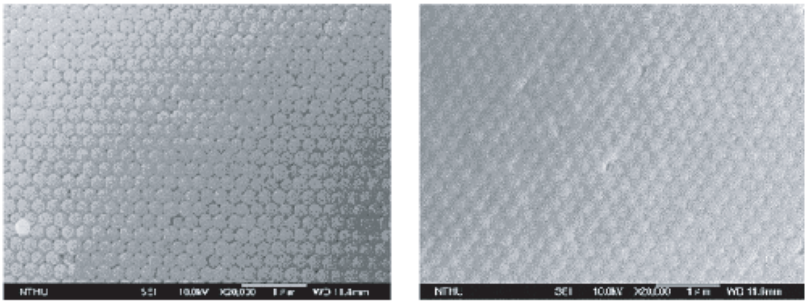

(a)

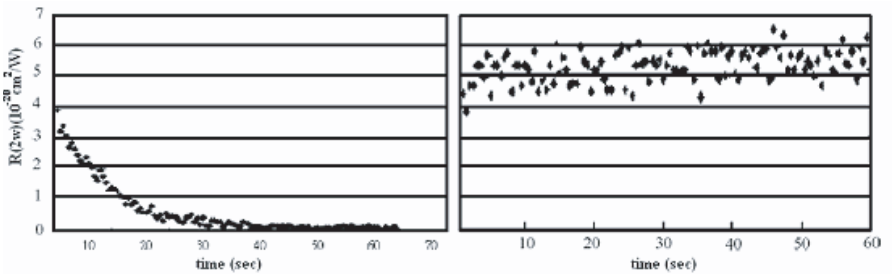

(b)

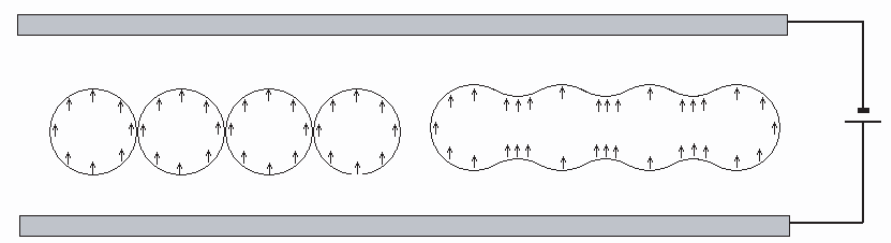

(c)

Fig. 11. Comparison of silica plates prepared after 4 days sintering at 1000 °C (left) and 1050 °C (right): (a) the SEM photographs, (b) the SHG reflectivity at an incident angle of 22.5°, (c) the polarized spheres in separated and close contact forms.

induce micro-charge separation. In this sense, electric potential induced by –OH groups on surfaces is enhanced by applying an electric field in conjunction with light irradiation, which can account for the second harmonic wave generated via the third-order susceptibility resulting from a coupling of two photons and the electrostatic field characterized by the Gouy-Chapman model. The vanishing of transmitted SH signals from the dehydrated silica are due to the loss of –OH groups on the particle surfaces.

In this scenario, silica micro-spheres have a large electro-optic coefficient, but only charges on the surface induced by the –OH groups play a role in generating the SHG via third-order susceptibility. To determine the large value of Pockel coefficient of silica micro-spheres, two additional experiments were performed. Firstly, silica spheres were sedimentary adhered to thin glass plates by a process of heat drying and densification [26]. The –OH groups on the surface are lost after thermal poling. The regular arrays of silica spheres (the left of Fig. 11a) become closely packed and intimately connected (the right of Fig. 11a) as the annealing temperature increases to 1050 °C. We have measured the reflected SHG from the thermally poled samples at an incident angle of 22.5°. The SH signal of the closely packed is five times larger and persistent in time than those of loosely packed sample as shown in Figure 11b. Silica glass after thermal poling exhibits a higher internal depletion field built into the interface between upper layers.

Furthermore, Maker fringes are displayed for a monolayer of dehydrated silica spheres under an electric field of 3×10^7 V/m as shown in Figure 12 with intensity normalized to an AT-cut quartz plate. The signal near normal incidence is zero, where surface charges were lost during dehydration. The intensities at other incident angles are much larger than that obtained from silica suspension indicating second-order nonlinearity, which is proportional to the linear Pockels coefficient confirming the large value of ATR measured r_{33}.

5 Conclusions

In summary, from the study of the linear and nonlinear optical properties of the μm sized silica micro-spheres under external fields for hydrated and dehydrated states, the properties of silica spheres in the liquid suspension and in the dehydrated state are very different. Dehydration

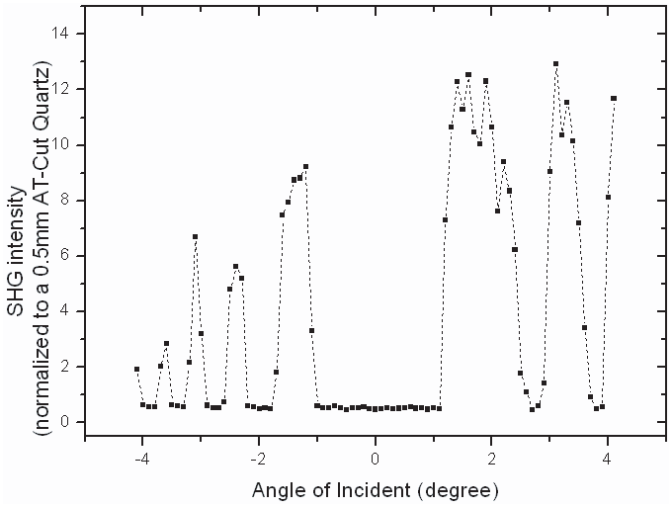

Fig. 12. Maker fringes for dehydrated silica spheres under an electric field of 3×10^7 V/m. The transmitted SHG is normalized from a normal incident SH beam of an AT-cut quartz crystal of thickness 0.5 mm with $d_{11} = 9.55 \times 10^{-10}$ esu.

seems irreversible for silica spheres. The migration of silica spheres in fluid under electric biasing addresses the dramatic shift of ATR dips for suspension. The dielectric constants of dehydrated silica spheres decrease slightly under electric polarization. The measured electro-optic coefficient, $r_{33} \sim 3.4 \pm 0.7$ pm/V, is about ten times larger than that obtained from the planar fused silica. A periodic dip within the typical ATR dip was observed, which should be of benefit for further studies of different structures. We have assumed that the macro-charge separation during the exposure of fundamental light under a bias is the main source for SHG. The transmitted SHG is attributed to surface potential, which is characterized by the Gouy-Chapman model.

References

1. U. Osterberg, W. Margulis, Opt. Lett. **11**, 516 (1986)
2. R.A. Myers, N. Mukherjee, S.R.J. Bruech, Opt. Lett. **16**, 1732 (1991)
3. V.L. Brudny, B.S. Mendoza, W.L. Mocha'n, Phys. Rev. B **62**, 11152 (2000)
4. W.L. Mochan, J.A. Maytorena, B.S. Mendoza, V.L. Brudny, Phys. Rev. B **68**, 085318 (2003)
5. J.I. Dadap, J. Shan, T.F. Heinz, J. Opt. Soc. Am. B. **21**, 1328 (2004)
6. Y. Pavlyukh, W. Hubner, Phys. Rev. B **70**, 245434 (2004)
7. H. Wang, E.C.Y. Yan, E. Borguet, K.B. Eisenthal, Chem. Phys. Lett. **259**, 15 (1996)
8. E.C. Yan, Y. Liu, K.B. Eisenthal, J. Phys. Chem. **102**, 6331 (1998)
9. N. Yang, W.E. Angerer, A.G. Yodh, Phys. Rev. Lett. **87**, 103902 (2001)
10. P. Galletto, P.F. Brevet, H.H. Girault, R. Antoine, M. Broyer, J. Phys. Chem. B **103**, 8706 (1999)
11. V. Boutou, C. Favre, Opt. Lett. **30**, 759 (2005)
12. H. Raether, *Surface Plasmons on Smooth and Rough Surfaces and on Gratings* (Springer, New York, 1988)
13. `http://www.luxpop.com/`
14. C.P. Pang, C.T. Hsieh, J.T. Lue, J. Phys. D: Appl. Phys. **36**, 1764 (2003)
15. A. Yariv, P. Yeh, *Optical Waves in Crystal*, Wiley Series in Pure and Applied Optics (Wiley, New York, 1984)
16. X. Zhao, S. Ong, K.B. Eisenthal, Chem. Phys. Lett. **202**, 513 (1993)
17. N.D. Denkov, O.D. Velev, P.A. Kralchevsky, I.B. Ivanv, H. Yoshimura, K. Nagayama, Nature, **361**, 26 (1993)
18. P. Jiang, J.F. Bertone, K.S. Hwang, V.L. Colvin, Chem. Mater. **11**(8), 2132 (1999)
19. C.S. Chang, J.T. Lue, Surf. Sci. **393**, 231 (1997)
20. X.-C. Long, R.A. Myers, S.R.J. Brueck, Opt. Lett. **19**, 1819 (1994)
21. R.L. Dong, T.S. Lin, J.T. Lue, J. Nonlin. Opt. Phys. Mat. **10**, 441 (2001)
22. L.R. Snyder, Sep. Sci. **1**, 191 (1966)
23. A. Agzamkhodzhaev, L.T. Zhuravlev, A.V. Kiselev, K.Y. Shengeliya, Kolloidn. Zh. **36**, 1145 (1974)
24. D. Carrol, X.H. Zheng, Pure Appl. Opt. **7**, L49 (1998)
25. J. Kasparian, B. Krämer, J.-P. Dewitz, S. Vadja, R. Rairoux, B. Vezin, V. Boutou, T. Leisner, W. Hübner, J.-P. Wolf, L. Wöste, K.-H. Bennemann, Phys. Rev. Lett. **78**, 2952 (1997)
26. Y.Q. Lue, T.K. Ho, C.P. Pang, J.T. Lue, J. Nonlin. Opt. Phys. Mat. **14**, 93 (2005)